Rev. Roum. Sci. Techn.– Électrotechn. et Énerg.
Vol. **62**, *4*, pp. 341–345, Bucarest, 2017

Électrotechnique et électroénergétique

THE SYNTHESIS OF CYLINDRICAL CONDUCTORS THROUGH PUNCTIFORMAL CHARGES AND APPLICATIONS

DAN MICU

Key words: Field synthesis, Electrical images, Capacitance, Earth electrodes.

The paper presents a method for replacing two cylindrical surfaces having a common axis, situated at the same potential, with a distribution of punctual charges placed on the common axis. This allows the computation of the capacitance of the two conductors, with applications in determining the resistance of the cylindrical earth electrode. The model is used in verifying the precision of a practical formula for these electrodes.

1. INTRODUCTION

Every problem in electromagnetic field synthesis [1, 2] starts with choosing the physical model and the mathematical model [3], followed by the determination of the numerical model, that is a linear system of equations of the form

$$A \cdot z = u \,. \tag{1}$$

If the number of equations is equal to the number of unknowns and the condition number [4] is not too large then direct computation can lead to acceptable solutions.

On the other hand, in most cases there are more equations than unknowns (overdetermined system) or fewer (under determined system). In these cases we apply methods that are specific to field synthesis to determine the minimum error solutions (the pseudo-solutions) and for each of these we find the solutions of minimal norm (the normal pseudo-solutions). The binomial coefficient method [5] is very effective in this stage of synthesis. If for physical reasons the solutions are not acceptable than we resort to regularization [6]. However, finding the optimal choice for the regularization parameter is still an open problem. Nevertheless, by taking the parameter on the elbow of the curve L (the curve plotting the norm of the solution against the norm of the error) we can achieve an acceptable balance between the precision and stability (satisfiability) of the solution.

The approach of replacing an equipotential surface that is symmetric with respect to the meridian plane with a distribution of punctual charges on the axis of symmetry has been tested [8] on simple surfaces, so that the result of synthesis was directly verified. On this ground, the case of a single cylinder is analyzed in [9]. Determining the image charges on the axis of symmetry was done here through the direct method, the binomial coefficient method and the regularization method. The results were used for computing the capacitance of a cylinder with respect to ground according to the ratio between the radius and the length of the cylinder. Thus, we have verified the practical formula [10, 11] for the capacitance of a cylinder. There exist, of course, other methods for approaching the subject of this paper [12–14] and we have verified the precision of a practical formula for spherical earth electrodes in another paper [15]. Unfortunately, the approach is only available for spherical and cylindrical symmetry [16].

2. COMPUTING THE IMAGE CHARGES AND CAPACITANCE FOR TWO CYLINDERS

We consider two disjoint cylindrical conductive bodies having the same rotational axis. We assume that the two bodies are at the same potential V, which is known. In Fig.1 we present a section through the two cylinders and the rotational axis Ox. The symmetrical part below the axis is not drawn.

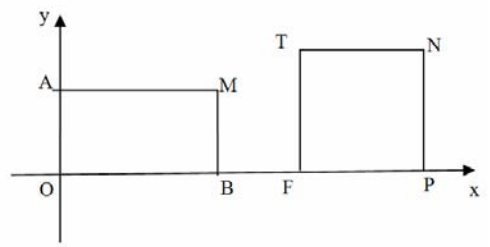

Fig. 1 – A section through the rotational cylinders.

Take OA = R, OB = h, FT = r and FP = H and let BF = g be the distance between the two cylinders.

The image charge inside the first cylinder will be found on the open segment OB in n–1 equidistant points, obtained by dividing the length h of the cylinder in n equal parts. We note the image charge on the point of abscisse kh/n by q_k, where k is between 1 and n–1.

The image charges inside the second cylinder will be found on the open segment FP in p–1 equidistant points, obtained by dividing the length H of the cylinder in p equal parts.

In the point of abscisse $h+g+(k–n+1)H/p$ we take, the currently unknown, image charge q_k with k between n and $n+p$–2, so we will have p–1 image charges inside the second cylinder.

We now divide the path OA-AM-MB in m equal parts with length $d = \dfrac{2R+h}{m}$. We note $[R/d] = a$ and $[(R+h)/d] = b$, where the bracket represents the floor function.

Thus, the points on OA will have coordinates $(0, jd)$ with j being a natural number in the closed interval $[0, a]$.

The points on AM will have coordinates $(jd–R, R)$ with j a natural number in the interval $(a, b]$.

The points on MB will have coordinates $(h, md–jd)$ with j a natural number in the interval $(b, m]$. In this way, the points on the path are taken in order, from O to A, M, B.

Technical University of Cluj-Napoca, Romania, E-mail d_o_micu@yahoo.com

We have an equation for every point of division, including the ends, so we obtain $m+1$ equations.

We now divide the path FT-TN-NP in q equal parts with length $D=\frac{2r+H}{q}$. We note $[r/D] = a$ and $[(r+H)/D] = f$.

Thus, the points on FT will have coordinates $(h+g, jD)$ with j being a natural number in the closed interval $[0, e]$.

The points on TN will have coordinates $(h+g+jD-r, r)$ with j a natural number in the interval $(e, f]$.

The points on NP will have coordinates $(h+g+H, qD-jD)$ with j a natural number in the interval $(f, q]$. When writting the equations j will be unique to the two cylinders, so that the intervals for j given above will be appropriately shifted.

In this way, the points on the outline of the second cylinder are taken in order, from F to T, N, P. We have an equation for every point of division, so we obtain $q+1$ additional equations. Thus the total number of equations is $m+q+2$, while the total number of unknowns is $n+p-2$.

For each of the $m+q+2$ points on the closed path given by the segments OA-AM-MB and FT-TN-NP respectively, we will write an equation representing the given potential V of the point, a potential that is determined by the $n-1$ unknown charges on the open segment OB and the $p-1$ unknown charges on the open segment FP.

We will have six different types of equations, depending on which segment is the point whose potential we compute situated.

Thus, for the points on OA, for $j = 0, 1, 2, \ldots, a$, we have $a+1$ equations of the form:

$$\sum_{k=1}^{n-1}\frac{\frac{q_k}{4\pi\varepsilon}}{\sqrt{\left(k\frac{h}{n}\right)^2+j^2d^2}}+ +\sum_{k=n}^{n+p-2}\frac{\frac{q_k}{4\pi\varepsilon}}{\sqrt{\left(h+g+(k-n+1)\frac{H}{p}\right)^2+j^2d^2}}=V. \tag{2}$$

For points on AM, for $j = a+1, a+2, \ldots, b$, we have $b-a$ equations of the form:

$$\sum_{k=1}^{n-1}\frac{\frac{q_k}{4\pi\varepsilon}}{\sqrt{\left(jd-R-k\frac{h}{n}\right)^2+R^2}}+ +\sum_{k=n}^{n+p-2}\frac{\frac{q_k}{4\pi\varepsilon}}{\sqrt{\left(h+g+(k-n+1)\frac{H}{p}-jd+R\right)^2+R}}=V. \tag{3}$$

For points on MB, for $j = b+1, b+2, \ldots, m$, we have $m-b$ equations of the form:

$$\sum_{k=1}^{n-1}\frac{\frac{q_k}{4\pi\varepsilon}}{\sqrt{\left(h-k\frac{h}{n}\right)^2+(md-jd)^2}}+ +\sum_{k=n}^{n+p-2}\frac{\frac{q_k}{4\pi\varepsilon}}{\sqrt{\left(g+(k-n+1)\frac{H}{p}\right)^2+(md-jd)^2}}=V. \tag{4}$$

We verify that the number of equations on this path is $a+1+b-a+m-b = m+1$.

For the points on the second cylinder it becomes difficult to ensure the continuity of j.

For points on FT, for $j = m+1, m+2, \ldots, m+e+1$, we have $e+1$ equations of the form:

$$\sum_{k=1}^{n-1}\frac{\frac{q_k}{4\pi\varepsilon}}{\sqrt{\left(h+g-k\frac{h}{n}\right)^2+(j-m-1)^2D^2}}+ +\sum_{k=n}^{n+p-2}\frac{\frac{q_k}{4\pi\varepsilon}}{\sqrt{\left((k-n+1)\frac{H}{p}\right)^2+(j-m-1)^2D^2}}=V. \tag{5}$$

For points on TN, for $j = m+e+2, m+e+3, \ldots, m+f+1$, we have $f-e$ equations of the form:

$$\sum_{k=1}^{n-1}\frac{\frac{q_k}{4\pi\varepsilon}}{\sqrt{\left((j-m-1)D+h+g-k\frac{h}{n}\right)^2+r^2}}+ +\sum_{k=n}^{n+p-2}\frac{\frac{q_k}{4\pi\varepsilon}}{\sqrt{\left((k-n+1)\frac{H}{p}-(j-m-1)D\right)^2+r^2}}=V. \tag{6}$$

For points on NP, for $j = m+f+2, m+f+3, \ldots, m+q+1$, we have $q-f$ equations of the form:

$$\sum_{k=1}^{n-1}\frac{\frac{q_k}{4\pi\varepsilon}}{\sqrt{\left(h+g+H-k\frac{h}{n}\right)^2+\left((m+q+1)D-jD\right)^2}}+ +\sum_{k=n}^{n+p-2}\frac{\frac{q_k}{4\pi\varepsilon}}{\sqrt{\left(H-(k-n+1)\frac{H}{p}\right)^2+\left((m+q+1)D-jD\right)^2}}=V. \tag{7}$$

We verify that the number of equations on the path of the second cylinder is $e+1+f-e+q-f = q+1$.

COMPUTATIONAL EXAMPLE. We take $R = 1$ m, $h = 4$ m, $r = 2$ m, $H = 5$ m, $g = 1$ m and $V = 1$ V (volt).

We choose $m = q = 10$ and $n = p = 12$. The number of equations is $m+q+2 = 22$. The number of unknowns is $n+p-2 = 22$.

The choice was made so that that the linear system can be directly solved, if permitted by the system's conditioning.

The computations are made in the MathCAD Software. The spectral condition number of the system's matrix $\boldsymbol{S}$ is $\text{cond2}(\boldsymbol{S}) = 5.05 \times 10^5$. This allows direct resolution of the

system. We mention that the directly calculated solution coincides with the normal pseudosolution of the system.

The unknown punctual charges are measured in nC (nanocoulomb), which leads to acceptable values of the elements of the system matrix $\boldsymbol{S}$: $s_{11} = 3$, $s_{12} = 1.5$, $s_{13} = 1$, $s_{21} = 1.457$, $s_{22} = 1.115$, $s_{23} = 0.857$, $s_{31} = 0.991$, $s_{32} = 0.906$, $s_{33} = 0{,}781$ etc.

The column matrix of the solution is noted $\boldsymbol{Q}$, the elements of this matrix being the wanted image charges, measured in nC: $q_1 = 0.064$, $q_2 = -1.131$, $q_3 = 5.42$, $q_4 = -12.089$, $q_5 = 16.32$, $q_6 = -15.017$, $q_7 = 10.364$, $q_8 = -5.522$, $q_9 = 2.07$, $q_{10} = -0.391$, $q_{11} = 0.021$, $q_{12} = 0.868$, $q_{13} = -11.887$, $q_{14} = 57.999$ etc.

If we note $\boldsymbol{W}$ the column matrix of free terms (which in this case has elements equal to 1/9) then the column matrix of the error is $\mathbf{Er} = \boldsymbol{S} \times \boldsymbol{Q} - \boldsymbol{W}$, with elements $er_1 = -9.731 \cdot 10^{-9}$, $er_2 = 9.836 \cdot 10^{-8}$, $er_3 = -1.676 \cdot 10^{-7}$, $er_4 = 5.679 \cdot 10^{-8}$ etc. The norm of the error matrix **Er** is $2.107 \cdot 10^{-7}$.

The capacitance of the system of two cylinders is computed with the formula:

$$C_{cap} = \frac{1}{V}\sum_{k=1}^{n+p-2} q_k = \frac{1}{V}\sum_{k=1}^{22} q_k \,, \tag{8}$$

giving the result is $C_{cap} = 0.343$ nF.

The capacitance of a single cylinder with $R = 1$ m and $h = 4$ m, calculated with the presented method in the case of absence of the second cylinder with $m = 10$ şi $n = 12$, leads to $C_1 = 0.174$ nF.

The capacitance of the second cylinder, calculated under hypothesis of absence of the first cylinder $r = 2$ m, $H = 5$ m, $m = 10$ and $n = 12$, leads to $C_2 = 0.282$ nF.

The two capacitors, placed in parallel, without mutual influence, give capacitance $C = C_1 + C_2 = 0.456$ nF.

The same result can be obtained if we take the distance g between the cylinders as very large.

It is interesting to follow the variation of the capacitance for progressively larger distances:

- for $g = 10$ m we have $C = 0.404$ nF,
- for $g = 20$ m we have $C = 0.423$ nF ,
- for $g = 30$ m we have $C = 0.432$ nF ,
- for $g = 40$ m we have $C = 0.437$ nF,
- for $g = 50$ m we have $C = 0.440$ nF .

In what follows the growth is slower, thus :

- for $g = 100$ m we only have $C = 0.447$ nF,
- for $g = 500$ m we have $C = 0.453$ nF, then
- for $g = 1\,000$ m we have $C = 0.454$ nF and only
- for $g = 2\,000$ m we reach $C = 0.455$ nF, where it remains for $g = 10{,}000$ m.

3. THE COMPUTATIONAL PRECISION FOR THE FORMULA FOR RESISTANCE OF A CYLINDRICALLY SHAPED EARTHED ELECTRODE

The cylindrical earth electrode consists in practice of a steel pipe with length between one and three meters and radius around a few centimeters [17, 18].

We consider a cylindrical earth electrode of radius R and length h that is buried vertically at a depth G (Fig. 2).

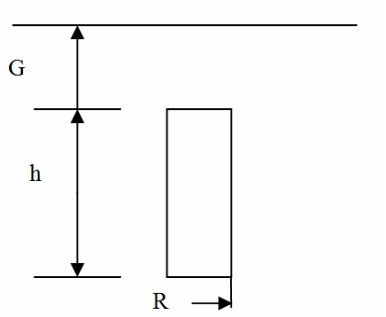

Fig. 2 – A cylindrical earth electrode, buried at depth G.

The exact computation of the distribution of potential created in the ground by such a socket (buried at great depth, that is with G infinite) leads to complicated formulas, that are inconvenient for practical use, due to the hybrid shape of the cylindrical socket: a cylindrical surface with two circular shaped plane surfaces at the end.

Under these conditions the cylindrical electrode is approximated to an oblong rotational ellipsoid [11], having big semiaxis equal to half of the given cylinder's length and small semiaxis equal to the cylinder's radius. This model becomes closer to reality the higher the ratio between the length and radius of the cylinder. Using the Laplace equation in the coordinate system of the oblong ellipsoid one finds the potential of the socket in an exterior point.

We then compute the electrical field and the current density. We integrate the current density on the surface of the ellipsoid and obtain the expression for the current dissipated by the outlet. The ratio between the potential of the outlet and this current gives the resistance of the cylindrical ground socket buried at large depth.

$$R_\infty = \frac{\rho}{2\pi h}\ln\frac{h}{R}\,. \tag{9}$$

To compute the resistance of the earth electrode buried at depth G we use the direct method. Taking into consideration the method of images from electrokinetics, Fig. 3, the scheme on the left of the figure becomes the one on the right, which assumes a homogenous environment of resistivity ρ and two cylinders situated symmetrical with respect to the point were before was the surface of the ground.

We consider the model from Fig. 3 from the right side and, using the formula for the outlet's potential [11], we calculate the outlet's own potential and add to it the potential created by the image outlet in a point situated in the middle of the given outlet.

We obtain formulas [10, 11], for the resistance of the earth electrode of cylindrical shape, of radius R and length h, buried vertically at depth G (Fig. 3).

$$R_p = \frac{\rho}{2\pi h}\ln\left(\frac{h}{R}\sqrt{\frac{h+4G}{3h+4G}}\right). \tag{10}$$

We remark that in proving formula (9) we needed the condition that the radius R of the outlet be a lot smaller than its length h.

We recall that in applying the direct method we have made another approximation: we have computed the potential given by the image cylinder in a single point of the given cylinder. These approximations will render the formula inaccurate, so that our approach in this chapter is legitimate.

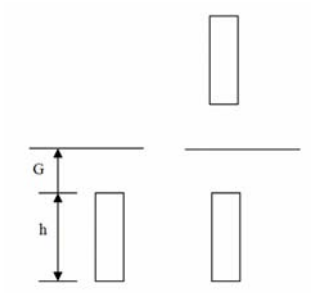

Fig. 3 – The earth electrode and the electrokinetic model.

In Table 1 we see the resistances of the ground socket R_p, computed using the formula (9). The columns represent different depths of burying for the socket, G = 1, 2, 3, 4 m, while on the rows the radius R of the cylinder varies in increments of 2 cm, up to 20 cm. The resistivity of the soil was taken to be ρ = 100 Ωm.

Tabel 1

	G = 1 m	G = 2 m	G =3 m	G =4 m
R = 2 cm	59.58	60.66	61.12	61.37
R = 4 cm	48.55	49.63	50.09	50.34
R = 6 cm	42.09	43.18	43.63	43.89
R = 8 cm	37.52	38.60	39.05	39.31
R = 10 cm	33.96	35.05	35.50	35.76
R = 12 cm	31.06	32.14	32.60	32.86
R = 14 cm	28.61	29.69	30.15	30.40
R=16 cm	26.48	27.57	28.02	28.28
R=18 cm	24.61	25.69	26.15	26.40
R=20 cm	22.93	24.01	24.47	24.73

The first observation refers to the fact that, contrary to our knowledge, the resistance of the outlet increases as the burying depth grows.

Let us remark that, if in the model considered in the preceding chapter we take $r = R$, $H = h$ and consider $g = 2G$, we obtain the electrostatic model that corresponds to the electrokinetic model on the right hand side of Fig. 3.

If we note the capacitance, expressed in nanofarads, according to the previous algorithm, with C[nF] and the passive resistance and passive conductance of the ground socket from Fig. 3 with R_t and G_t respectively, we get:

$$R_t = \frac{1}{G} = \frac{1}{\frac{1}{2}\cdot\frac{\sigma}{\varepsilon}C[\mathrm{nF}]} = 2\varepsilon\rho\frac{1}{C[\mathrm{nF}]} = \frac{100}{18\pi C[\mathrm{nF}]}. \quad (11)$$

We present in Table 2 the values of the passive resistance corresponding to the ones in Table 1, computed with the method proposed in the previous section.

Tabel 2

	G = 1 m	G = 2 m	G = 3 m	G = 4 m
R = 2 cm	39,86	38,63	38,15	37,89
R = 4 cm	37,84	37,35	36,98	36,61
R = 6 cm	36,45	36,02	35,76	35,13
R = 8 cm	35,41	34,30	33,84	33,59
R = 10 cm	31,85	30,73	30,27	30,01
R = 12 cm	31,31	29,68	29,21	28,96
R = 14 cm	30,15	29,04	28,57	28,32
R = 16 cm	28,88	27,77	27,31	27,05
R = 18 cm	27,41	26,30	25,84	25,58
R = 20 cm	26,01	24,91	24,44	24,19

To evaluate the precision of formula (9) we attach the relative error table [19], computed with:

$$\mathrm{er} = \frac{R_p - R_t}{R_t}. \quad (12)$$

Tabel 3

	G = 1 m	G = 2 m	G = 3 m	G = 4 m
R = 2 cm	49.5%	57.0%	60.2%	61.9%
R = 4 cm	28.3%	32.8%	35.4%	37.5%
R = 6 cm	15.4%	19.8%	22.0%	24.9%
R = 8 cm	5.9%	12.5%	15.4%	17.0%
R = 10 cm	6.6%	14.,1%	17.3%	19.2%
R = 12 cm	-0.8%	8.3%	11.6%	13.5%
R = 14 cm	-5.1%	2.2%	5.5%	7.3%
R = 16 cm	-8.3%	-0.7%	2.6%	4.5%
R = 18 cm	-10.2%	-2.3%	1.2%	3.2%
R = 20 cm	-11.8%	-3.6%	0.12%	2.2%

By comparing the results in the two tables we observe more significant differences in the case of smaller cylindric radii (*i.e.* close to 2 cm) than for radii of 10 cm or larger.

Thus, it is specifically at the ordinary values that the approximative formula gives more significant errors. At constant dimension of the cylinder, as burying depth increases, the error of the formula does the same. This is another major inconvenience, because in practical circumstances the burying depth is larger than 1 m.

4. CONCLUSIONS

Replacing cylindrical conductive surfaces with punctual charges is an electromagnetic field synthesis problem. We remark that the problem, though ill-conditioned, leads to a system of equation whose condition number is not too large, which allows for a direct solution of the system. An immediate application of the two cylinder problem refers to verifying the precision of a formula used in practice for computing the passive resistance of the earth electrode. We observe the large errors entailed by this formula. In comparison with the exact value of the earth electrode's resistance, the values given by the formula are much higher.

Thus, while the use of the formula does not produce electrical accidents, it causes an unjustified increase in costs of the grounding installation.

Received on 21 August, 2017

REFERENCES

1. A.N. Tihonov, V.I. Arsenin, *Méthodes de résolution de problèmes mal posés*, Edition MIR, Moscou, 1974.
2. A. Ţugulea, *Câteva sinteze de câmp magnetic în regim staţionar*, Studii şi cercetări energetice şi electrotehnice, **14**, *4*, 1964.
3. F.I. Hantila, T. Leuca, C. Ifrim, *Electrotehnica teoretică*, Edit. Electra, 2002.
4. Adriana Micu, D. Micu, N. Patachi, *Le nombre de condition*, Rev. Roum. Sci. Techn. – Électrotechn. et Énerg., **44**, *2*, pp. 121–134, 1999.
5. D. Micu, *Contributions à la synthèse du champ électromagnétique par la méthode de régularisation des systèmes dégénérés*, Rev. Roum. Sci. Techn. – Électrotechn. et Énerg., **38**, *2*, pp. 169–179, 1993.

6. D. Micu, Adriana Micu, *Elemente de sinteza câmpului electromagnetic*, Edit. Dacia, Cluj-Napoca, 2003.
7. P.C. Hansen, *Analysis of discrete ill-posed problems by means of the L-curve*, SIAM Review, **34**, pp. 561–580, 1992.
8. D. Micu, Denisa Stet, D.D. Micu, *Synthesis method validation for electric image charges determination*, EMES, Oradea, 1–2 June, 2017.
9. D. Micu, Denisa Stet, *Computation of conductive cylinder images charges using synthesis method*, MPS, Cluj-Napoca, 8–10 June, 2017.
10. C. Mocanu, *Teoria campului electromagnetic*, Edit. Tehnică, Bucharest, 1979.
11. O. Centea, *Prizele de pământ din instalaţiile electrice*, Edit. Academiei Române, Bucharest 2006.
12. F.I. Hantila, G. Preda, M. Vasiliu, *Polarization method for state fields*, IEEE Trans. on Magn., **36**, *4*, pp. 672–675, 2000.
13. Marilena Stanculescu, M. Maricaru, F.I. Hantila, S. Marinescu, L. Bandici, *An iterative finite element-boundary element method for efficient magnetic field computation in transformers*, Rev. Roum. Sci. Techn. – Électrotechn. et Énerg., **44**, *3*, pp. 267–276.
14. D. Micu, *Numerical synthesis of electrostatic field by Monte Carlo method*, IEEE Trans. on Magn., **29**, pp. 1966–1969, 1993.
15. D. Micu, V. Popescu, D.D. Micu, Adriana Micu, *Precizia unor formule aproximative folosite la calculul prizelor de pământ*, SNET, Bucharest, 2009.
16. T. Micu, D. Micu, *Geometrie elementară în electrotehnica teoretică*, Edit. Didactică şi Pedagogică, Bucharest, 2016.
17. M. Duminicatu, C. Bianchi, C. Ionescu, N. Mironescu, *Proiectarea instalaţiilor de joasă tensiune*, Edit. Tehnică, Bucharest, 1975.
18. C. Mereuţă, J. Gayraud, *Măsuri practice pentru creşterea siguranţei în funcţionare a instalaţiilor energetice industriale*, Edit. Tehnică, Bucharest, 1980.
19. R. Munteanu, G. Todoran, *Teoria si practica prelucrarii datelor de masurare*, Edit. Mediamira, Cluj-Napoca, 1997.